Molecular Recognition of Carbohydrates by Zinc Porphyrins: Lewis Acid/Lewis Base Combinations as a Dominant Factor for Their Selectivity

Tadashi Mizutani,* Takuya Kurahashi, Takeshi Murakami, Noriyoshi Matsumi, and Hisanobu Ogoshi*

Contribution from the Department of Synthetic Chemistry and Biological Chemistry, Graduate School of Engineering, Kyoto University, Sakyo-ku, Kyoto 606-01, Japan

Received April 25, 1997. Revised Manuscript Received July 8, 1997[⊗]

Abstract: A systematic study of the binding of carbohydrates by functionalized zinc porphyrins indicated that [5, 15-bis(8-quinolyl)porphyrinato]zinc(II) (**1**) showed marked affinity for octyl glucoside and mannoside in $CHCl_3$ ($-\Delta G^\circ = 4.5-6.3$ kcal mol^{-1}). Analysis of the complexation-induced shifts of the carbohydrate OH protons in the ^{1}H NMR revealed that receptor **1** bound the 4-OH group of mannoside and glucoside by coordination to the zinc and the 6-OH and 3-OH groups by hydrogen bonding to the quinolyl nitrogen atoms. These NMR results and comparison of binding affinity with reference receptors and ligands indicated that receptor **1** recognized the *trans*,*trans*-1,2-dihydroxy-3-(hydroxymethyl) moiety of carbohydrates by the combination of Lewis acid (zinc) and Lewis bases (quinolyl nitrogens). Poor affinities of **1** to octyl galactosides and octyl 2-*O*-methyl-α-mannoside were ascribed to neighboring group effects, where a neighboring group in ligands not directly involved in the receptor−ligand interactions had considerable influence on the affinity through destabilizing the hydrogen-bonding-network(s) in the receptor−ligand complex. The circular dichroism induced in the porphyrin Soret band by complexation with the carbohydrates displayed characteristic patterns, which parallel the patterns of the complexation-induced shifts in the ^{1}H NMR. The CD patterns sensitively reflected the receptor−ligand interaction modes, particularly ligand orientation and fluctuation in the complex. Variable-temperature CD revealed that glucoside was fluctuating on **1** while mannoside was rigidly fixed on **1** at room temperature. Addition of alcohols to $CHCl_3$ suppressed the binding by **1**, while addition of polar additives such as water, alcohols, phenols, and ethers assisted the binding by **3** and **4** ($-\Delta\Delta G^\circ = 0.2-0.4$ kcal mol^{-1}) in a low concentration range (0−1.5 mol %).

Among a number of carbohydrates, glucose, galactose, mannose, fucose, *N*-acetylglucosamine, *N*-acetylgalactosamine, and sialic acids are known to play key roles in the cell recognition. Precise molecular recognition of these carbohydrates by a synthetic receptor is a challenging goal in artificial receptor chemistry. Considerable efforts have been done to construct model receptors of sugars, including resorcinolaldehyde cyclotetramer,[1] tetrahydroxycholaphane,[2] C_3 macrocyclic receptor,[3] boronic-acid-based receptors,[4] polyaza cleft,[5] aminocyclodextrins,[6] phosphonates,[7] capped porphyrin,[8] glycophane,[9] and polypyridine macrocycle.[10] These studies focused on diverse aspects of carbohydrate recognition such as diastereoselectivity, enantioselectivity, binding in polar solvents, and facile detection of the binding events, particularly by taking advantage of the chirality of carbohydrates. Owing to the structural similarity of carbohydrates and their highly polar nature, we are still far from the goal, particularly specific carbohydrate recognition in water via noncovalent interactions. Another important aspect of carbohydrate recognition chemistry is that carbohydrates are poor substrates for spectroscopic investigations. Therefore, it is desired to develop a sensitive spectroscopic method to probe the carbohydrate binding.

The X-ray crystallographic structure of the mannose-binding protein−mannose complex showed that calcium and carboxylates of the amino acid side chains form hydrogen-bonding-networks with mannose.[11] To mimic such hydrogen-bonding-networks, we designed receptors bearing two hydrogen-bonding sites and one Lewis acid site fixed on porphyrins.[12] We aim to address the following two issues: (1) the structural motif of receptors required for carbohydrate recognition and structural features of carbohydrates to be recognized by the receptors and (2) roles of polar additives in energetics and selectivity of carbohydrate recognition, based on the comparative studies of binding affinity, ^{1}H NMR, and induced circular dichroism studies of the relative orientation of ligands in the receptor−ligand complexes.

Results

Five zinc porphyrins were prepared, and their affinities for carbohydrate derivatives were investigated. Receptor **1** has two

[⊗] Abstract published in *Advance ACS Abstracts,* September 15, 1997.

(1) (a) Aoyama, Y.; Tanaka, Y.; Sugahara, S. *J. Am. Chem. Soc.* **1989**, *111*, 5397. (b) Kurihara, K.; Ohto, K.; Tanaka, Y.; Aoyama, Y.; Kunitake, T. *J. Am. Chem. Soc.* **1991**, *113*, 444.

(2) Bhattarai, K. M.; Bonar-Law, R. P.; Davis, A. P.; Murray, B. A. *J. Chem. Soc., Chem. Commun.* **1992**, 752.

(3) Liu, R.; Still, W. C. *Tetrahedron Lett.* **1993**, *34*, 2573.

(4) (a) Murakami, H.; Nagasaki, T.; Hamachi, I.; Shinkai, S. *Tetrahedron Lett.* **1993**, *34*, 6273. (b) James, T. D.; Sandanayake, K. R. A. S.; Shinkai, S. *Nature* **1995**, *374*, 345. (c) James, T. D.; Sandanayake, K. R. A. S.; Iguchi, R.; Shinkai, S. *J. Am. Chem. Soc.* **1995**, *117*, 8982. (d) Takeuchi, M.; Imada, T.; Shinkai, S. *J. Am. Chem. Soc.* **1996**, *118*, 10658.

(5) Huang, C.-Y.; Cabell, L. A.; Anslyn, E. V. *J. Am. Chem. Soc.* **1994**, *116*, 2778.

(6) Eliseev, A. V.; Schneider, H.-J. *J. Am. Chem. Soc.* **1994**, *116*, 6081.

(7) Das, G.; Hamilton, A. D. *J. Am. Chem. Soc.* **1994**, *116*, 11139.

(8) Bonar-Law, R. P.; Sanders, J. K. M. *J. Am. Chem. Soc.* **1995**, *117*, 259.

(9) Jimenez-Barbero, J.; Junquera, E.; Martin-Pastor, M.; Sharma, S.; Vicent, C.; Penades, S. *J. Am. Chem. Soc.* **1995**, *117*, 11198.

(10) Inouye, M.; Miyake, T.; Furusyo, M.; Nakazumi, H. *J. Am. Chem. Soc.* **1995**, *117*, 12416.

(11) Weis, W. I.; Drickamer, K.; Hendrickson, W. A. *Nature* **1992**, *360*, 127.

(12) For preliminary accounts of this work, see: Mizutani, T.; Murakami, T.; Matsumi, N.; Kurahashi, T.; Ogoshi, H. *J. Chem. Soc., Chem. Commun.* **1995**, 1257.

S0002-7863(97)01318-8 CCC: $14.00 © 1997 American Chemical Society

Table 1. Binding Constants (K) and Free Energy Changes ($\Delta G°$) of Receptor−Carbohydrate Complex Formation in Chloroform at 15 °C[a]

	K/M^{-1} ($-\Delta G°$/(kcal mol^{-1}))				
ligand	receptor **1**	receptor **2**	receptor **3**	receptor **4**	receptor **5**
α-Glc	7 570 (5.11)	2 530 (4.49)	320 (3.30)	3 670 (4.70)	<10 (<1.3)
β-Glc	41 400 (6.09)	6 360 (5.01)	570 (3.63)	2 090 (4.38)	440 (3.49)
α-Gal	1 870 (4.31)	1 030 (3.97)	650 (3.70)	2 240 (4.42)	14 (1.51)
β-Gal	3 840 (4.73)	1 620 (4.23)	690 (3.74)	1 710 (4.26)	<10 (<1.3)
α-Man	15 500 (5.52)	8 220 (5.16)	810 (3.83)	3 860 (4.73)	695 (3.75)
β-Man	61 700 (6.31)	23 300 (5.76)	250 (3.16)	2 970 (4.58)	78 (2.49)
2-*O*-Me-α-Man	380 (3.40)	250 (3.16)	400 (3.43)	2 550 (4.49)	*b*
6-*O*-Ac-β-Glc	6800 (5.05)	2060 (4.37)	530 (3.59)	*b*	*b*
6-*O*-Bz-β-Glc	7300 (5.09)	*b*	600 (3.66)	*b*	*b*

[a] Standard deviations in K are about 5−10%. [b] Not determined.

quinolyl groups fixed at the 5- and 15-positions of porphyrin with a cis configuration, receptor **3** has two 2-hydroxynaphthyl groups with a cis configuration, and receptor **4** has two 2,7-dihydroxynaphthyl groups with a trans configuration. All these

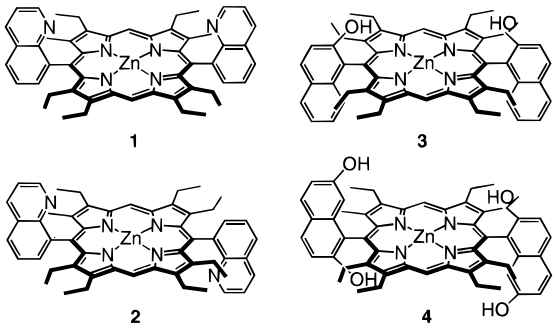

porphyrins have one Lewis acid site and two hydrogen-bonding sites arranged in a similar manner to form a recognition pocket above the porphyrin plane. Receptor **2** is the trans isomer of receptor **1**, serving one Lewis acid site and one hydrogen-bonding site for carbohydrate binding. Receptor **5**, ZnTPP (TPP = 5,10,15,20-tetraphenylporphyrinato anion), has only one Lewis acid site. Receptor **2** and receptor **5** were used in control experiments to reveal the influence of the quinolyl hydrogen-bonding sites.

We used chloroform as a solvent for the binding studies to mimic the relatively nonpolar environment of the binding pocket of sugar-binding proteins. The effects of polar additives were examined by adding them to the chloroform. To solubilize the carbohydrates in organic solvents, we prepared octyl pyranosides according to reported procedures. Four octyl glycopyranosides, namely, α- and β-octyl galactopyranoside (α- and β-Gal), α- and β-octyl mannopyranoside (α- and β-Man) thus prepared and two commercially available octyl pyranosides, α- and β-octyl glucopyranoside (α- and β-Glc), were used as ligands. As reference ligands, octyl 2-*O*-α-D-methylmannopyranoside (2-*O*-Me-α-Man), octyl 6-*O*-β-D-acetylglucopyranoside (6-*O*-Ac-β-Glc), and octyl 6-*O*-β-D-benzoylglucopyranoside (6-*O*-Bz-β-Glc) were prepared.

Binding Constants Determinations by UV−Vis Titration. The binding constants were determined by UV−vis titration, in which the absorbance changes in the Soret band owing to the increased ligand concentration were monitored and analyzed by least-squares curve fitting, assuming a 1:1 complex formation. In all cases, the Soret peak maxima were red-shifted by *ca.* 5 nm, and the difference spectra showed isosbestic points. The curve fitting to 1:1 complexation was satisfactory (standard deviations for the binding constants were *ca.* 5%).

The binding constants of octyl pyranosides and those of the reference ligands **6**−**13** are listed in Tables 1 and 2, respectively.

Table 2. Binding Constants (K) and Free Energy Changes ($\Delta G°$) for Complexation of Porphyrin Receptors **1** (or **3**) with Reference Ligands in Chloroform at 15 °C[a]

	K/M^{-1} ($-\Delta G°$/(kcal mol^{-1}))	
ligand	receptor **1**	receptor **3**
6	3 (0.63)	3 (0.63)
7	3 (0.63)	19 (1.68)
8	5 (0.92)	17 (1.62)
9	7 (1.11)	5 (0.92)
10	210 (3.05)	140 (2.80)
11	60 (2.32)	43 (2.15)
12	2600 (4.50)	320 (3.29)
13	560 (3.62)	88 (2.56)

[a] In amylene-containing $CHCl_3$. [**1**] = 5.4×10^{-6} to 7.4×10^{-6} M, [**3**] = 4.6×10^{-6} to 5.8×10^{-6} M, [**6**−**9**] = 0−3.4×10^{-1} M, [**10**−**13**] = 0−9.6×10^{-3} M.

Among the receptors investigated, receptor **1** showed the highest affinity for the ligands, especially for β-Man and β-Glc. A

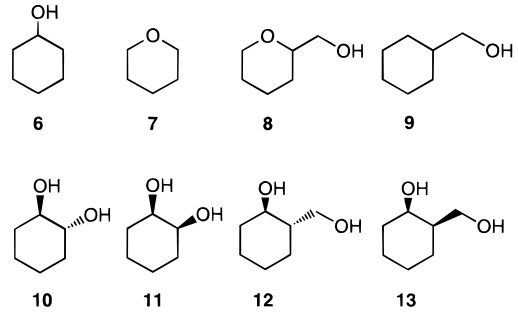

similar trend was found for the affinity of **2**, even though the affinity was reduced for all of the ligands compared to that of **1**. Binding by receptor **4** was moderate, and that by receptor **3** was weak. Comparison of the binding constants of α-Man with those of 2-*O*-Me-α-Man indicated that the 2-*O*-methyl group of 2-*O*-Me-α-Man markedly inhibited the binding by receptors **1** and **2** while it hardly influenced that by receptors **3** and **4**.

^{1}H NMR Study of Binding. The complexation-induced shifts (CIS) of the 1-H, 2-OH, 3-OH, 4-OH, and 6-OH resonances of α- and β-anomers of Glc, Man, and Gal were determined in $CDCl_3$ in the low-concentration range of receptor **1**. The assignments of the resonances of the four hydroxy protons were made on the basis of ^{1}H−^{1}H COSY or PDQF experiments. The observed chemical shifts were the average values of the free and the complexed ligand in the limit of fast chemical exchange. Figure 1 shows the ^{1}H NMR spectra of β-Man in the presence of varying amounts of receptor **1** in $CDCl_3$. Upon addition of **1**, the resonance for the 6-OH proton moved downfield and those for the 1-H, 3-OH, and 4-OH protons moved upfield. The signal for the 2-OH proton was hardly influenced at all upon complexation. The spectral changes in the resonances of the β-Glc protons were similar to

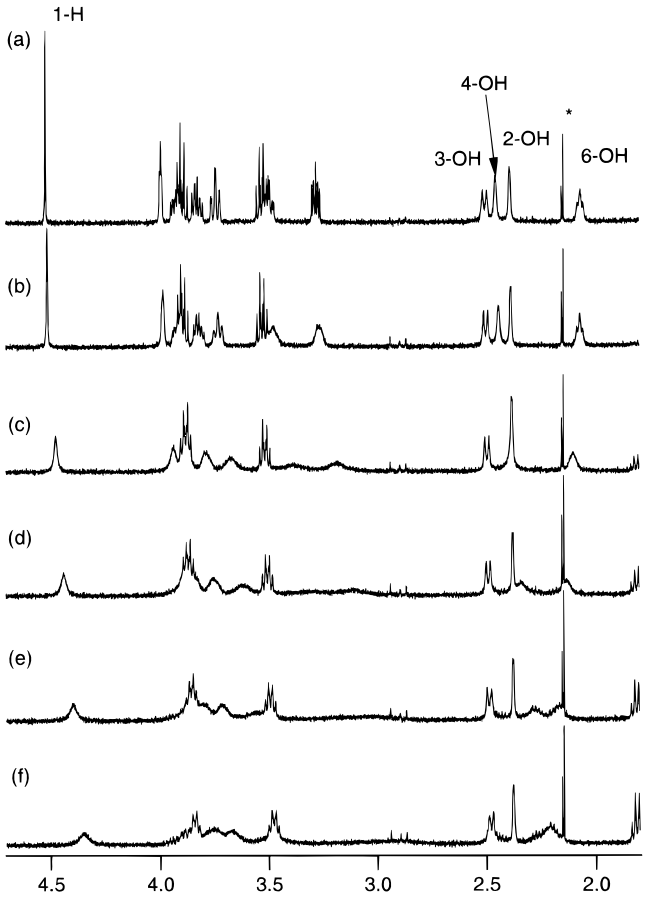

Figure 1. The ^{1}H NMR spectra of $CDCl_3$ solutions of β-Man in the presence of receptor **1** at 25 °C. (a) 0%, (b) 0.4%, (c) 2.5%, (d) 4.7%, (e) 6.8%, and (f) 8.9% of β-Man was complexed with receptor **1**.

Table 3. ^{1}H NMR Complexation-Induced Shifts (CIS, $\Delta\delta$/ppm) of β-Man, β-Glc, and β-Gal upon Addition of **1** in $CDCl_3$ at 25 °C[a]

	$\Delta\delta$/ppm (δ of free ligand/ppm)		
	β-Man	β-Glc	β-Gal
1-H	−2.1 (4.53)	−1.8 (4.29)	−3.8 (4.25)
2-OH	0.0 (2.38)	−0.1 (2.38)	−0.9 (2.37)
3-OH	−0.3 (2.50)	−1.5 (2.63)	−2.6 (2.60)
4-OH	−2.7 (2.45)	−2.2 (2.52)	−0.5 (2.76)
6-OH	+1.6 (2.06)	+1.2 (1.97)	−0.5 (2.08)

[a] Extrapolated to 100% complex from the CIS values at 0−25% complexation. Signal assignments were made on the basis of the ^{1}H−^{1}H COSY or PDQF experiments.

those of the β-Man protons. For β-Gal, the resonances associated with all these protons were shifted upfield. The values of CIS were linearly increased as the fraction of the ligand complexed with the receptor was increased, and the CIS values for the complex are determined by extrapolation to 100% complexation and listed in Tables 3 and 4. Similarly, the values of CIS of β-Glc, β-Man, and β-Gal by receptor **2** were determined and are listed in Table 5.

Induced Circular Dichroism (ICD) Study of Binding. Induced circular dichroism was observed in the Soret band of porphyrin receptors for some combinations of receptors and ligands. In Figure 2, the CD spectra of the **1**−β-Man complex and the **1**−β-Glc complex are shown. Although both β-Glc and β-Man were strongly bound to receptor **1**, the two ICD spectra were quite different. The **1**−β-Man complex showed biphasic Cotton effects (Figure 2a) while the **1**−β-Glc complex showed very weak Cotton effects (Figure 2b). Table 6 summarizes the values of $\Delta\epsilon$ for each complex, where the CD spectra were recorded under the conditions that 30−95% of the

Table 4. ^{1}H NMR Complexation-Induced Shifts (CIS, $\Delta\delta$/ppm) of α-Man, α-Glc, and α-Gal upon Addition of **1** in $CDCl_3$ at 25 °C[a]

	$\Delta\delta$/ppm (δ of free ligand/ppm)		
	α-Man	α-Glc	α-Gal
1-H	−1.6 (4.83)	−1.5 (4.85)	−2.2 (4.94)
2-OH	+0.9 (2.20)	+0.3 (1.96)	+0.6 (1.88)
3-OH	−1.8 (2.40)	−2.2 (2.52)	−3.4 (2.52)
4-OH	−2.4 (2.36)	−2.0 (2.44)	−1.7 (2.79)
6-OH	+1.4 (1.99)	+0.4 (1.88)	+0.5 (2.20)

[a] Extrapolated to 100% complex from the CIS values at 0−25% complexation. Signal assignments were made on the basis of the ^{1}H−^{1}H COSY or PDQF experiments.

Table 5. ^{1}H NMR Complexation-Induced Shifts (CIS, $\Delta\delta$/ppm) of β-Man, β-Glc, and β-Gal upon Addition of **2** in $CDCl_3$ at 25 °C[a]

	$\Delta\delta$/ppm (δ of free ligand/ppm)		
	β-Man	β-Glc	β-Gal
1-H	−1.0 (4.53)	−1.2 (4.29)	−1.5 (4.24)
2-OH	−0.3 (2.38)	−0.4 (2.36)	−1.3 (2.35)
3-OH	−0.3 (2.47)	−1.4 (2.60)	−0.8 (2.58)
4-OH	−2.0 (2.42)	−2.2 (2.48)	−0.6 (2.75)
6-OH	+0.3 (2.03)	+0.2 (1.95)	+0.1 (2.06)

[a] Extrapolated to 100% complex from the CIS values at 0−25% complexation. Signal assignments were made on the basis of ^{1}H−^{1}H COSY experiments.

receptor was complexed and the values of $\Delta\epsilon$ were corrected for the fractions of complexed porphyrin receptors. The ICD patterns induced in **1**−**3** by α-anomers were similar to those by β-anomers for Glc, Man, and Gal. The signal intensities of the ICD of **1** decrease in the order, Man ≫ Gal ≈ Glc. High affinity for Glc and the very small Cotton effects induced by it are indications that the intensity of Cotton effects is not related to the binding affinity. The different ICD between Man and Glc indicates that the stereochemistry at C-2 carbon has significant effects on the ICD. In order to further investigate the effects of substituents at C-2 on the ICD, the CD spectrum of the 2-*O*-Me-α-Man was recorded. Interestingly, the Cotton effects were nearly diminished ($|\Delta\epsilon| < 5$). Although receptors **3** and **4** showed weak affinity for the ligand, some complexes showed Cotton effects with comparable intensity to those of the **1**−Man complex. For instance, the receptor **3**−Glc complex showed distinct Cotton effects even though the binding was weak.

The CD spectra were also recorded for some of the complexes at low temperatures, to −60 °C, in $CHCl_3$. The Cotton effects for both the receptor **1**−α-Man complex and the receptor **1**−α-Glc complex were increased with lower temperatures. The CD spectra for these complexes are shown in Figure 3. The **1**−α-Glc complex exhibited biphasic Cotton effects at −60 °C similar to those of the **1**−α-Man complex. The **1**−β-Glc complex also exhibited similar biphasic ICD at −60 °C (data not shown). Both the **1**−α-Gal complex and the **1**−β-Gal complex showed biphasic Cotton effects at −60 °C with an opposite sign (negative Cotton effects at 414 nm and positive Cotton effects at 421 nm).

Solvent Effects on the Binding. Sanders *et al.*[8] reported that the addition of water and methanol to the chloroform solution assists the binding of carbohydrate derivatives by the capped zinc porphyrin. We also examined the effects of polar additives on the binding of carbohydrates. The free energy changes of binding of β-Glc, $-\Delta G°$, are plotted against the mole fractions of added alcohols in Figures 4 and 5. For receptor **1**, the binding was simply inhibited as the concentration of alcohols in $CHCl_3$ was higher. On the other hand, for receptor **4**, the values of $-\Delta G°$ increased in the range of the low alcohol

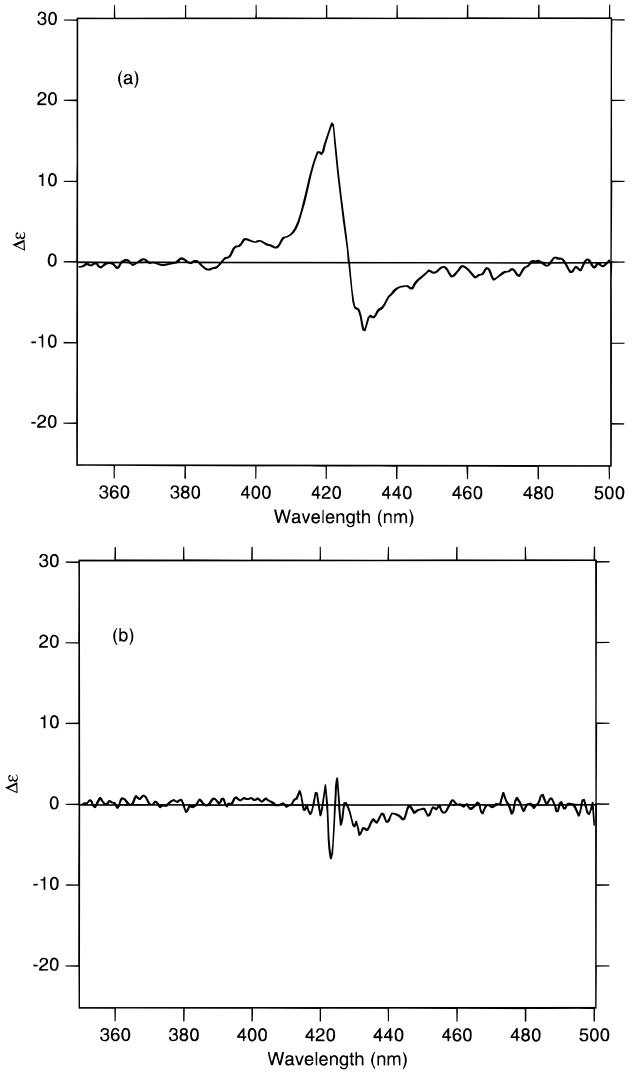

Figure 2. Circular dichroism induced in receptor **1** by (a) β-Man and (b) β-Glc in $CHCl_3$ at 15 °C. [**1**] = 6.51 × 10^{-6} M, [β-Man] = 5.36 × 10^{-3} M, [β-Glc] = 1.22 × 10^{-2} M.

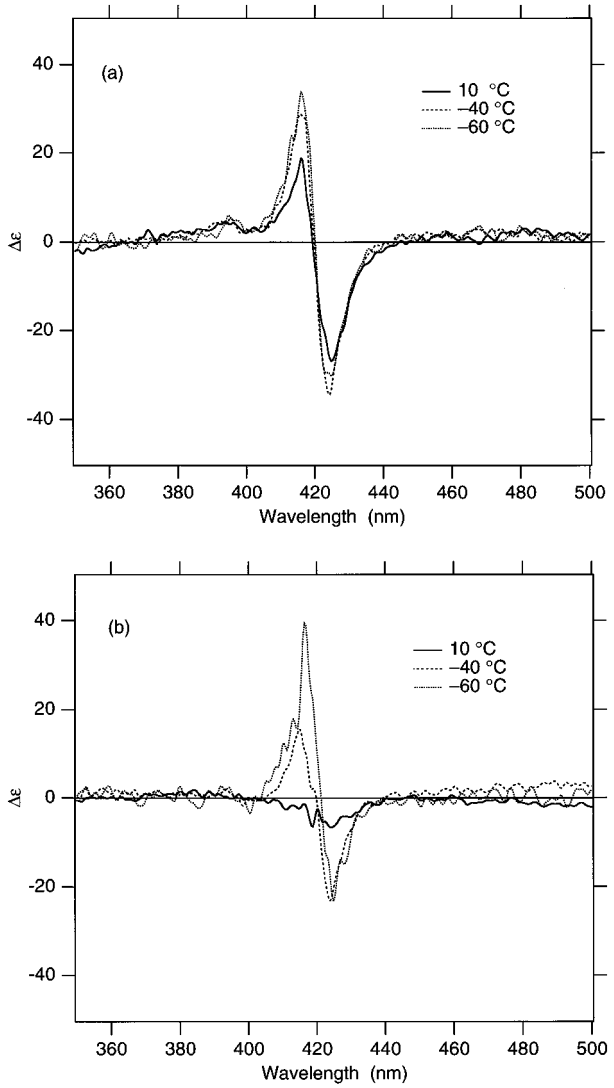

Figure 3. Circular dichroism induced in receptor **1** by (a) α-Man and (b) α-Glc at 10, −40, and −60 °C in $CHCl_3$. (a) [**1**] = 5.21 × 10^{-6} M, [α-Man] = 6.31 × 10^{-3} M, (b) [**1**] = 5.21 × 10^{-6} M, [α-Glc] = 1.87 × 10^{-3} M.

Table 6. Differential Dichroic Absorption ($\Delta\epsilon$) of Receptor−Carbohydrate Complexes in Chloroform at 15 °C

	$\Delta\epsilon$/(cm^{-1} M^{-1}), (wavelength/nm)				
ligand	receptor **1**	receptor **2**	receptor **3**	receptor **4**	receptor **5**[b]
α-Glc	*a*	−8 (423)	18 (418) −18 (428)	18 (418) −9 (433)	*a*
β-Glc	*a*	−8 (425)	20 (420) −10 (430)	5 (420) −3 (435)	*a*
α-Gal	*a*	*a*	*a*	11 (420)	*a*
β-Gal	*a*	*a*	*a*	−5 (420)	*a*
α-Man	22 (420) −26 (426)	6 (416) −13 (427)	18 (418) −24 (438)	−13 (428)	*a*
β-Man	18 (422) −6 (432)	7 (416) −6 (427)	17 (418) −12 (436)	−5 (420)	*a*
2-*O*-Me-α-Man	*a*	*a*	−10 (410) 13 (421)	−19 (417)	

[a] $|\Delta\epsilon| < 5$ in 400−450 nm. [b] ZnTPP.

concentration and decreased upon further addition of alcohol. In Figure 6, the similar plots are shown for complexation of β-Glc to **3** for the various additives such as water, phenol, *p*-nitrophenol, *p*-methoxyphenol, *p*-dimethoxybenzene, and pyridine. Water showed very distinct effects: the binding constant increased rapidly in the low concentration range of water until the chloroform became saturated. *p*-Dimethoxybenzene and *p*-methoxyphenol also showed distinct effects in the low-concentration range. Other phenols showed moderate effects. In contrast, addition of pyridine simply suppressed the binding.

The effects of added alcohols on the induced CD of the receptor−ligand complexes were examined. For most of the complexes examined, effects of the additives on the ICD were too small to observe. In the complex between **3** and β-Glc, however, the values of $|\Delta\epsilon|$ at 427 nm distinctly increased with increasing the *tert*-butyl alcohol concentrations up to 7 mol %: $\Delta\epsilon$, cm^{-1} M^{-1}(^{t}BuOH, mol %) −10 (0), −15 (0.75), −21 (2.2), −25 (7.1) at 427 nm. Since the binding constants were decreased beyond 1.5 mol % of *tert*-butyl alcohol, the signal intensity of ICD was increased in the concentration range where the binding constants were decreasing. These results indicate that *tert*-butyl alcohol did interact with the receptor−ligand complex and altered the interaction modes to some extent.

Discussion

Receptor Design. Receptors **1**, **3**, and **4** all have three interaction sites for carbohydrates, one Lewis acid site (Zn) in common, and two hydrogen-bonding sites, namely, hydrogen acceptors (N) in **1** and hydrogen donors (OH) in **3** and **4**. We reported previously that **3** and **4** selectively bound amino acid esters with a polar side chain, dimethyl aspartate, and dimethyl

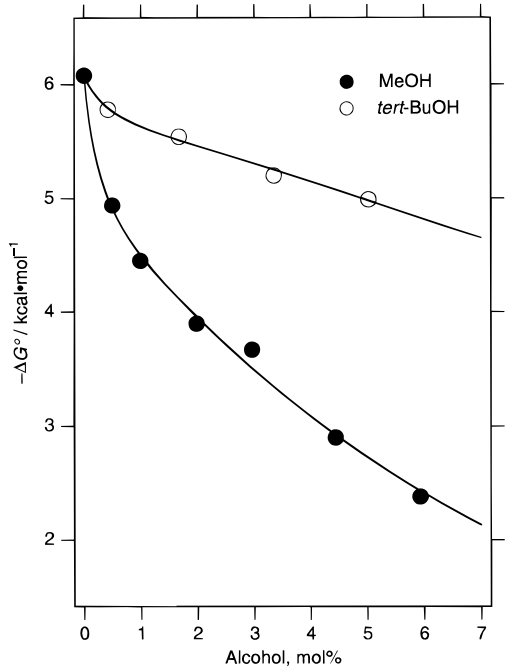

Figure 4. Plot of the free energy changes for complexation between receptor **1** and β-Glc in $CHCl_3$ at 15 °C ($-\Delta G°$) against alcohol concentrations.

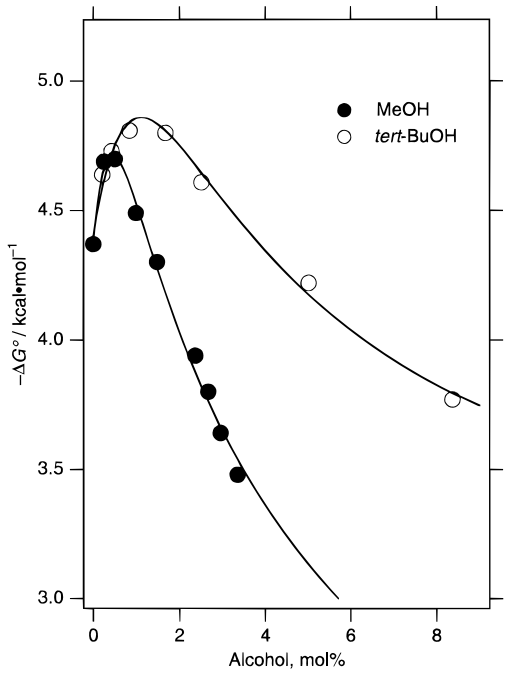

Figure 5. Plot of the free energy changes for complexation between receptor **4** and β-Glc in $CHCl_3$ at 15 °C ($-\Delta G°$) against alcohol concentrations.

glutamate.[13] For carbohydrates, however, receptors **1** and **2** showed better affinity and selectivity than **3** and **4**, showing the importance of the hydrogen acceptor/donor combinations for carbohydrate recognition. The Lewis base/Lewis acid/Lewis base combination in **1** formed a better binding site than the Lewis acid/Lewis acid/Lewis acid combination in **3** and **4**. For comparison of selectivity, the differences in $-\Delta G°$ between the most strongly bound pyranoside ligand and the most weakly bound ligand are 2.9 kcal/mol for **1**, 0.6 kcal/mol for **3**, and 0.4 kcal/mol for **4**, confirming that the selectivity is highest for

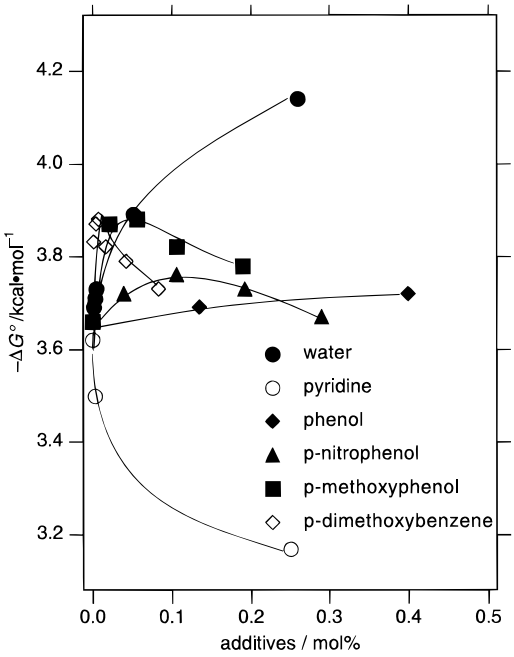

Figure 6. Plot of the free energy changes for complexation between receptor **3** and β-Glc in $CHCl_3$ at 15 °C ($-\Delta G°$) against concentrations of water, phenol, *p*-nitrophenol, *p*-methoxyphenol, *p*-dimethoxybenzene, and pyridine.

receptor **1**. Receptor **2**, the trans isomer of **1**, showed a similar pattern of binding affinity but weaker in magnitude. Therefore, the two quinolyl groups with the cis configuration in **1** cooperatively assisted the binding of the ligands. When the zinc of receptor **1** was replaced with two protons, the free base of **1** showed much reduced affinity for carbohydrates. For instance, the binding constant for β-Glc was *ca*. 600 M^{-1}.[14] This confirms the important role of the zinc. Both the Lewis acid site and the Lewis base sites are needed to bind carbohydrates strongly.

Carbohydrate Selectivity of Receptors 1 and 2. Receptor **1** showed high affinity for both mannosides and glucosides rather than galactosides. The stereochemical arrangement of C-5, C-4, and C-3 of Glc is the same as that of Man, and this arrangement was particularly well recognized by receptor **1**. Gal, the epimer of Glc at C4, was weakly bound, indicating that the stereochemistry at C4 was crucial. In contrast, the stereochemistry at C2 was less important. For the stereochemistry at C1, β-anomers were bound more strongly to receptor **1** than the corresponding α-anomers of Man, Glc, and Gal. The trend of these affinities suggests that, in the **1**−Man complex and the **1**−Glc complex, the 4-OH group was directly involved in the receptor−ligand interaction, while the 2-OH group was not.

As simpler analogs of carbohydrates, the affinities for cyclohexanediols **10**−**13** were determined (Table 2). Comparison between the binding constant of **10** and that of **11** indicates that the trans vicinal dihydroxy configuration was favored over the cis configuration by receptor **1**. Similarly, comparison of the binding constant between **12** and **13** indicates that the trans vicinal hydroxy hydroxymethyl configuration was favored over the cis configuration.

NMR Study for Determination of Interacting Hydroxy Groups. Since receptor **1** has three interaction sites while the pyranoside ligands have four OH groups, it is important to determine which OH groups directly interact with the receptor. The ^1H NMR chemical shift displacements for carbohydrate OH

(13) Mizutani, T.; Murakami, T.; Kurahashi, T.; Ogoshi, H. *J. Org. Chem.* **1996**, *61*, 539.

(14) Owing to the small changes in absorbance in visible spectra, the precise determination of binding constants was difficult.

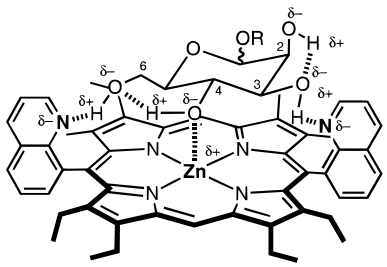

Figure 7. Schematic representation of hydrogen-bonding-networks of the receptor **1**−Man complex based on the ^{1}H NMR CIS values.

protons induced by complexation with porphyrin receptors were found to provide valuable information. Two opposing anisotropic effects should be taken into account to interpret the CIS values of ligand upon complexation with porphyrin receptors: an upfield shift due to the ring current of porphyrin when the ligand proton is located above the porphyrin plane in the center and a downfield shift of the OH protons upon hydrogen bonding. Effects of the ring current of quinolyl groups were estimated to be small except for the hydrogen-bonding protons to the quinolyl nitrogen, based on the isoshielding map.[15]

Table 3 indicates that Man and Glc show similar patterns of the sign of the CIS values, while Gal shows a different trend. The resonance for the 6-OH proton was shifted downfield, and that for the 4-OH proton was shifted upfield for both Man and Glc. These CIS values indicate that it is indeed the 4-OH group that is coordinated to the zinc and the 6-OH group that is hydrogen bonded to the quinolyl nitrogen (see Figure 7). In this hydrogen-bonding-network, an alternating charge arrangement, Zn(δ+)−4O(δ−)−4-*O*-H(δ+)−6O(δ−)−6-*O*-H(δ+)−N(δ−), is achieved, which, we suggest, particularly stabilizes the **1**−Man complex and the **1**−Glc complex. The X-ray crystallographic study of Ca^{2+}-dependent lectin showed that mannoside was bound via a hydrogen-bonding-network involving calcium, glutamate, and aspartate.[16] The binding mode of receptor **1** toward mannoside was thus similar, zinc in place of calcium and quinolyl groups in place of carboxylates.

If the receptor **1**−Man (Glc) complexes adopt this bidentate binding mode, then the 3-OH group is located close to the other quinolyl nitrogen and can form a hydrogen bond to it. For Man, the 2-OH group can assist the intermolecular hydrogen bonding between the 3-OH group and the quinolyl nitrogen by the intramolecular hydrogen bonding to the 3-OH group as shown in Figure 7. Anslyn *et al.*[5] demonstrated the importance of intramolecular hydrogen bonding in polyols recognition and pointed out that *cis*-cyclohexanediol forms stronger intramolecular hydrogen bonding than the trans diol. Therefore, the intramolecular hydrogen bonding between the 2-OH group and the 3-OH group of Man should be stronger than that of Glc. The resonance for the 3-OH proton of Man appeared downfield from that of Glc in the complex (Table 3). This is consistent with the intramolecular hydrogen-bonding-network shown in Figure 7, because the stronger hydrogen bonding between the 3-OH group of Man and the quinolyl nitrogen should cause greater downfield shift of this proton than the 3-OH proton of Glc. The CD spectroscopic studies at low temperatures also support the above discussion as described later in this paper. The higher affinity for Man than Glc can also be accounted for by this intramolecular hydrogen bonding.

The CIS patterns for Gal were different from those of Man and Glc with respect to the signs of CIS of the 6-OH resonance and the magnitude of CIS of the 4-OH resonance. The axial 4-OH in Gal should make the hydrogen-bonding-network shown in Figure 7 unfeasible. The upfield shift of the 6-OH group of galactose indicates that there was no strong hydrogen bonding between the 6-OH group and the quinolyl nitrogen in the complex. Among the OH protons of Gal, the greatest upfield shift was observed for the resonance of the 3-OH proton, rather than that of the 4-OH proton. This suggests that the 3-OH group was coordinated to the Zn.

Comparison of binding affinities to reference ligands **10**−**13** indicates that *trans*-1,2-dihydroxy moiety was favored over the cis moiety, and *trans*-1,2-(hydroxymethyl)hydroxy moiety favored over the cis moiety. The high affinity to Man and Glc with the 4-OH coordination to the zinc of receptor **1** and the low affinity to Gal with the 3-OH coordination to the zinc are thus consistent with the affinity of **1** to the reference ligands.

Receptor **2**, the trans isomer of **1**, also showed characteristic CIS patterns. For both β-Man and β-Glc, the greatest upfield shifts were observed for the 4-OH resonances, thus suggesting that the 4-OH group was coordinated to the Zn. The difference in the CIS patterns of **2** from those of receptor **1** was that the downfield shifts of the 6-OH resonance were almost diminished and the shifts of the 2-OH resonance and of the 3-OH resonance remained unchanged. Thus, the quinolyl nitrogen of **2** chose the 3-OH group rather than the 6-OH group of Man and Glc as a hydrogen-bond donor.

Lewis Acid/Lewis Base Arrangements in Receptors and Ligands and Neighboring Group Participation. The binding constants of 2-*O*-Me-α-Man for receptor **1** and receptor **2** were reduced by a factor of 30−40 compared to α-Man. The alkylation of the 2-OH group not directly involved in the hydrogen-bonding interaction between receptor **1** and Man dramatically suppressed the binding. One can explain, however, this trend by assuming that the methoxy group prevents the original intramolecular hydrogen donation from the 2-OH group to the 3-OH group, and rather, the lone-pair electrons of the 2-methoxy group have repulsive interaction with the developing negative charge on the 3-OH group upon hydrogen bonding to the quinolyl nitrogen. For receptors **3** and **4**, which have acidic OH groups in place of basic quinolyl nitrogen, the binding of 2-*O*-Me-α-Man was reduced only by a factor of at most 2 compared with that of α-Man. This different behavior of receptor **3** and receptor **4** also supports the above mechanism, that is, for receptor **1**, the combination of basic nitrogen and the 2-methoxy group adjacent to the hydrogen-bonding hydroxy group leads to significant destabilization of the complex.

A similar explanation is possible for the low affinity of **1** to galactosides. The ^{1}H NMR study showed that **1** recognized the trans vicinal hydroxy groups of Gal, *i.e.*, the 2-OH and 3-OH groups, by binding the 3-OH group via the zinc and the 2-OH group via the quinolyl nitrogen. The 1-octyloxy group then comes next to the hydrogen-bonding 2-OH group. The repulsion between this alkoxy group and the 2-OH group hydrogen bonded to the quinolyl nitrogen would lead to the low affinity for galactosides. These neighboring group effects are summarized in Figure 8. The OH group α to the hydrogen-donating OH group assists the binding by neutralizing the negative charge on the oxygen upon hydrogen bonding, while the alkoxy group at the same position inhibits it by destroying the hydrogen-bonding-network.

The upfield shift of the 2-OH proton of β-Gal upon addition of **2** indicated that the 2-OH group was coordinated to the Zn. The 2-OH coordination of β-Gal rather than the 3-OH coordination can be ascribed to the neighboring group inhibition shown in Figure 8, where the 3-OH coordination would lead to the

(15) Johnson, C. E. J.; Bovey, F. A. *J. Chem. Phys.* **1958**, *29*, 1012.
(16) Weis, W. I.; Drickamer, K.; Hendrickson, W. A. *Nature* **1992**, *360*, 127.

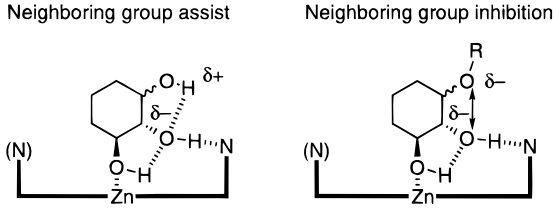

Figure 8. Common structural motif of Man, Gal, and 2-*O*-Me-α-Man interacting receptors **1** and **2**. Left: neighboring OH group assists the binding by neutralizing the negative charge on the oxygen of the OH group hydrogen bonded to the quinolyl nitrogen. Right: neighboring alkoxy group inhibits the binding by the negative charge repulsion between the lone pair electrons of the alkoxy group and the hydrogen-bonding OH group.

unfavorable geometry. These results suggest that Lewis acid/Lewis base combinations of receptors and ligands involving both directly interacting substituents and their neighboring substituents are important for the binding selectivity.

Comparison of Induced Circular Dichroism in Porphyrin Soret Band by Carbohydrates with That by Amino Acid Esters. We have reported that chiral amino acid esters induced characteristic biphasic CD in the Soret band of porphyrin receptor upon ditopic binding.[17] L-Amino acid esters consistently induced biphasic CD in the Soret band with positive Cotton effects at higher energy and negative Cotton effects at lower energy. We also pointed out the importance of the carbonyl chromophore in the induced CD.[18] The relative orientation of the carbonyl group to porphyrin was suggested to determine the ICD pattern. In contrast to amino acid esters, carbohydrates have five chiral carbons; thus, diverse patterns of ICD are expected. We found that the patterns of the ICD again sensitively reflect receptor−ligand binding modes. The magnitudes of Cotton effects for carbohydrate complexes were comparable or weaker than those for amino acid ester complexes: the values of $|\Delta\epsilon|$ of the ICD for the complexes between receptors **1**−**5** and carbohydrates were 0−26 cm^{-1} M^{-1}, while those for the complexes between trans isomer of **3**, [*trans*-5, 15-bis(2-hydroxy-1-naphthyl)porphyrinato]zinc, and amino acid esters were 10−65 cm^{-1} M^{-1}.

Mechanism of Induced CD. The distinct biphasic CD induced in receptor **3** by Glc is contrasting with the weak CD signal induced in receptor **1** by the same ligand. When the small binding constant for receptor **3**−Glc complexes is considered, this observation evidently indicates that the ICD reflects the interaction modes such as relative orientations of the ligand to the receptor and the number of stable receptor−ligand configurations and not the binding affinity.

As shown in Table 6, the ICD patterns of complexes with receptor **2** were similar to those of the corresponding complexes with receptor **1**, although the magnitudes were reduced, showing that combination of zinc and only one quinolyl nitrogen was able to induce the observed ICD pattern, and the second quinolyl nitrogen in **1** had only secondary effects on the ICD. This is in accordance with the ^{1}H NMR CIS patterns, which also indicated that both **1** and **2** bind Glc and Man in a similar fashion via the 4-HO···Zn coordination and the 3-OH···N hydrogen bonding. Among the zinc porphyrin−amino acid ester complexes, only ditopic binding (Zn···NH_2 and OH···O=C) lead to distinct biphasic ICD. The fact that both **1** and **2** showed similar ICD patterns for Man and Glc indicates that ditopic

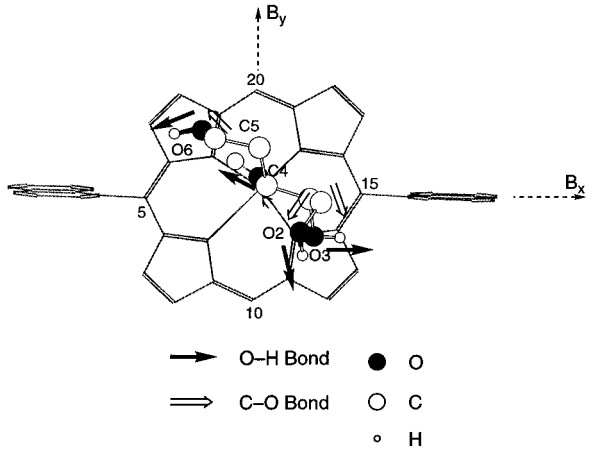

Figure 9. Directions of the C−O bonds and the O−H bonds of the 3-OH, 4-OH, and 6-OH groups for the receptor **1**−*β*-Man complex. The geometry is based on the PM3 calculations where Zn of receptor **1** is replaced by Al and the ethyl groups are by hydrogen. In the figure, hydrogens are omitted for clarity except for the OH protons. C1 and O5 of the ligand are also omitted.

fixation of the ligand in a similar fashion (4-HO···Zn and 3-OH···N) would determine the ICD patterns.

It is noteworthy that α-Man and *β*-Man induced biphasic CD in **1**, while α-Glc and *β*-Glc induced very weak CD at 15 °C, although both carbohydrates were bound strongly to **1**. Thus, the stereochemistry at the C2 position had significant influence on the induced CD pattern and intensity. The ^{1}H NMR studies revealed that the 2-OH group of Man and Glc was not involved in the direct hydrogen bonding with receptors **1** and **2**. We can ascribe the different ICD between Man and Glc to the following two mechanisms: (1) the coupling of the local wave function of the 2-OH group with that of porphyrin causes the different ICD and (2) the 2-OH group indirectly affects the binding mode to lead to the different ICD. One important observation for the mechanism of induced CD is that the receptor **1**−α-Glc complex showed only weak Cotton effects at 15 °C but distinct biphasic Cotton effects at −60 °C (Figure 3b). This ICD pattern was similar to that of the **1**−Man complex. Considering the similar ^{1}H NMR CIS patterns between the **1**−Man complex and the **1**−Glc complex, one can ascribe the weak ICD for the receptor **1**−α-Glc complex at room temperature to the thermal fluctuations. In contrast, the ICD of the **1**−Man complex was less sensitive to temperature (Figure 3a), possibly owing to the stronger 3-OH···N hydrogen bond.

If the hydrogen-bonding-network in the receptor **1**−Man complex, as schematically depicted in Figure 7, is assumed, then the orientation of the O−H bond and the C−O bond would be fixed relative to the porphyrin. Any deviation of the orientation of the transition dipole moments from the 5−15 axis and the 10−20 axis would contribute to the CD, and their sum would lead to the observed ICD if each contribution does not cancel each other. Figure 9 displays the geometry of the **1**−Man complex according to the molecular orbital calculations, in which one can see that the directions of these bonds are deviated from the axis. Although prediction of the bond directions is beyond the precision of the calculations, the figure suggests that the complex becomes optically active in terms of the directions of these bonds, provided that the ligand is fixed on the porphyrin plane.

These results evidently demonstrate that ICD is the powerful tool to probe the binding modes in the porphyrin−carbohydrate complexes such as ligand orientation and its fluctuation in the complex. It would be more powerful in investigation of

(17) Mizutani, T.; Ema, T.; Yoshida, T.; Kuroda, Y.; Ogoshi, H. *Inorg. Chem.* **1993**, *32*, 2072.
(18) Mizutani, T.; Ema, T.; Yoshida, T.; Renne, T.; Ogoshi, H. *Inorg. Chem.* **1994**, *33*, 3558.

polysaccharide recognition, where its ^{1}H NMR spectra are much more complicated and less useful for probing receptor−ligand structures.

Induced CD Probing Binding Modes. The following examples display that the receptor−ligand interaction modes are deduced from their ICD spectra: (1) The ICD patterns of α-Man and 2-*O*-Me-α-Man were similar for **4**, while they were different for **1** and **3**. Particularly, the signs of the CD induced in receptor **3** by α-Man were reversed of that induced by 2-*O*-Me-α-Man. Therefore, one can expect that the binding mode of the **3**−α-Man complex is different from that of the **3**−2-*O*-Me-α-Man complex. (2) It is interesting to note the differences in ICD between α- and *β*-anomers: the patterns of CD induced by the α-anomers in **1**−**3** were similar to those induced by the corresponding *β*-anomers, while those induced by α-anomers in **4** were different from those induced by the corresponding *β*-anomers. Particularly, the opposite sign of the Cotton effects of **4**−α-Gal to that of **4**−*β*-Gal indicates that α-Gal and *β*-Gal were bound to **4** in a different fashion. Therefore, the stereochemistry at C1 did not affect the ICD of **1**−**3**, while it affected the ICD of **4**. Although the binding constants by **4** of α-anomers were similar to those of *β*-anomers, the binding mode was different, possibly due to the longer distance between the zinc atom and the OH group in **4**.

Effects of Polar Additives on the Binding. In the binding pocket of lectins, water often participates in the hydrogen-bonding-network to stabilize the sugar−receptor complex. The role of a water molecule in the hydrophobic environment in thermodynamics of the interaction is thus an interesting problem.[19] In our model systems, polar additives showed different effects on the complex formation depending on whether receptors have basic recognition sites (**1**) or acidic recognition sites (**3** and **4**). Only inhibition of binding was observed for receptor **1**, while promoting effects of binding by water, alcohols, phenols, and ethers were observed for receptor **3** and receptor **4**. The ICD signals of **3**−*β*-Glc complex grew with increasing *tert*-butyl alcohol concentrations, indicating that *tert*-butyl alcohol did interact with the complex to stabilize it.[20]

To elucidate the effects of the steric factors and acidity of the OH group of the additives on the binding constants, the free energy changes in binding ($-\Delta G°$) in the presence of water, methyl alcohol, *tert*-butyl alcohol, phenol, *p*-nitrophenol, *p*-methoxyphenol, and *p*-dimethoxybenzene were compared (Figures 4−6). Both of methyl alcohol and *tert*-butyl alcohol showed the promoting effects on the binding, suggesting that steric demand was not severe. The stronger effects of *p*-methoxyphenol than those of *p*-nitrophenol and phenol indicate that acidity of the OH group is not the major factor for the present effects. Distinct effects of *p*-methoxyphenol and *p*-dimethoxybenzene strongly suggest that the ether group assists the binding. Here again, acid/base combination seems to play important roles. The assistance by the methoxy group of the additives implies that, for the host with three Lewis acidic sites, the Lewis basic methoxy group accepts hydrogen from the complex to form hydrogen-bonding-network among the receptor, the ligand, and the additive.

Conclusions. The binding affinities of a series of receptors determined by UV−vis titration experiments indicated that, for diastereoselective recognition of carbohydrates, the binding pocket of receptor **1** consisting of Lewis base/Lewis acid/Lewis base was found to be effective. The comparison of the affinity for a series of receptors and ligands, and the ^{1}H NMR and circular dichroism study revealed that receptor **1** with this binding pocket recognized the *trans*,*trans*-1,2-dihydroxy-3-(hydroxymethyl) moiety of carbohydrate through the zinc site and two quinolyl sites. Receptor **2**, in which only one quinolyl nitrogen and zinc can interact with ligands, the 1,2-*trans*-dihydroxy moiety was preferentially recognized. The patterns of induced CD parallel those of the CIS in the ^{1}H NMR spectra, suggesting that ICD was a facile probe to elucidate the binding mode. Variable temperature CD study demonstrated that Glc was fluctuating in receptor **1** at 15 °C, while Man was comparatively fixed in the binding pocket of **1** even at 15 °C. Low affinity of **1** for 2-*O*-Me-α-Man, α-Gal, and *β*-Gal suggests that the neighboring alkoxy group has considerable inhibitory effects on the binding. Addition of alcohols and ethers simply suppressed the binding by **1**, while it assisted the binding by **3** and **4**. In the complex between acidic receptors (**3** and **4**) and the ligands, Lewis basic ethers would assist the formation of hydrogen-bonding-networks. The intramolecular and intermolecular hydrogen-bonding-networks formed in the binding pocket markedly affected the selectivity of binding, and their control is the key to the design of receptor for carbohydrates.

Experimental Section

Instrumentation. ^{1}H and ^{13}C NMR spectra were recorded using a JEOL A-500 spectrometer in chloroform-*d* and DMSO-d_6, respectively. ^{1}H NMR chemical shifts in $CDCl_3$ were referenced to $CHCl_3$ (7.24 ppm), and ^{13}C NMR chemical shifts in DMSO-d_6 were reported relative to DMSO (39.5 ppm). UV−vis spectra were recorded on a Hewlett-Packard 8452 diode array spectrometer equipped with a thermostated cell compartment. Circular dichroism spectra were recorded on either a JASCO J-600 or a JASCO J-720 spectropolarimeter. A cryostat (Oxford, DN1704) was used for CD spectral measurements at low temperatures. Mass spectra were obtained using a JEOL JMS SX-102A mass spectrometer.

Materials. Ether and THF were distilled from sodium benzophenone ketyl radical. Pyridine, DMF, toluene, DMSO, and CH_2Cl_2 were distilled from CaH_2. Benzoyl chloride was distilled from $CaCl_2$. Acetyl chloride was distilled from P_2O_5. Methanol and ethanol were dried by refluxing with and distilling from magnesium. Octanol was distilled from sodium. Cyclohexene was distilled just before use. Acetic acid was dried by refluxing with acetic anhydride in the presence of 0.2% of 2-naphthalenesulfonic acid as a catalyst and was then fractionally distilled. Acetic anhydride was refluxed with and distilled from magnesium. *cis*- and *trans*-(2-Hydroxymethyl)cyclohexanol were prepared according to the reported procedure.[21] Materials for spectroscopic studies were obtained as follows. $CHCl_3$ containing amylenes as a stabilizer was purchased from Aldrich (A.C.S. HPLC grade, 99.9%, stabilized with amylenes) and was used as received. HPLC-grade water and spectrophotometric-grade methyl alcohol were used as received. *tert*-Butyl alcohol was dried by refluxing with and distilling from sodium. *p*-Nitrophenol, phenol, *p*-methoxyphenol, and *p*-dimethoxybenzene were completely dried under reduced pressure just before use, and their purity was checked by elemental analysis to avoid the influence by water contamination. Unless otherwise noted, other materials were obtained from commercial sources and used without further purification.

Receptors and Carbohydrates. [*cis*-5,15-Bis(2-hydroxy-1-naphthyl)-2,3,7,8,12,13,17,18-octaethylporphyrinato]zinc(II) (**3**) and [*trans*-

(19) (a) Miller, D. M., III.; Olson, J. S.; Pflugrath, J. W.; Quiochio, F. A. *J. Biol. Chem.* **1980**, *255*, 2465. (b) Miller, D. M., III.; Olson, J. S.; Pflugrath, J. W.; Quiochio, F. A. *J. Biol. Chem.* **1983**, *258*, 13665. (c) Bourne, Y.; Rouge, P.; Cambillau, C. *J. Biol. Chem.* **1990**, *265*, 18161.

(20) To examine how ligand aggregation affects the dependence of *K* on additive concentration, we compared the behaviors of **1** and **3**. Even though the binding constants were determined in the same concentration range of *β*-Gal, the binding constant between **3** and *β*-Gal increased while that between **1** and *β*-Gal simply decreased with increasing *tert*-butyl alcohol concentration, suggesting that the effects of *tert*-butyl alcohol cannot be ascribed to the dissolution of aggregate of *β*-Gal. The increased CD band by the addition of *tert*-butyl alcohol to the **3**−*β*-Glc complex also indicates that the effects of additives were due to the interaction between the additive and the complex.

(21) Gaunitz, S.; Schwarz, H.; Bohlmann, F. *Tetrahedron* **1975**, *31*, 185.

(22) Aoyama, Y.; Kamohara, T.; Yamagishi, A.; Toi, H.; Ogoshi, H. *Tetrahedron Lett.* **1987**, *28*, 2143.

5,15-bis(2,7-dihydroxy-1-naphthyl)-2,3,7,8,12,13,17,18-octaethylporphyrinato]zinc(II) (**4**) were prepared according to the published procedure.[23] Assignments of ^{1}H NMR signals were done by ^{1}H−^{1}H COSY or ^{1}H−^{1}H PDQF experiments.

Synthesis of [*cis*- and *trans*-5,15-Bis(8-quinolyl)-2,3,7,8,12,13,17,18-octaethylporphyrinato]zinc(II). It was synthesized according to the reported procedure.[22]

8-Formylquinoline. 8-Methylquinoline (1.46 g, 10 mmol) and selenium dioxide (1.3 g, 12 mmol) were mixed, and the suspension was stirred for 2 h at 160 °C. After the suspension was cooled to room temperature, the reaction mixture was poured to saturated aqueous $NaHCO_3$ and extracted with dichloromethane. The organic layer was dried over K_2CO_3 and evaporated. The residue was recrystallized from ethanol to obtain 8-formylquinoline (367 mg, 23%): ^{1}H NMR (500 MHz, $CDCl_3$) δ 11.46 (d, J = 0.9 Hz, 1H), 9.07 (dd, J = 4.3, 1.5 Hz, 1H), 8.35 (dd, J = 7.3, 1.5 Hz, 1H), 8.26 (dd, J = 8.3, 1.5 Hz, 1H), 8.11 (dd, J = 8.3, 1.5 Hz, 1H), 7.70 (dd, J = 7.3, 7.3 Hz, 1H), 7.53 (dd, J = 8.6, 4.3 Hz, 1H).

***cis*- and *trans*-5,15-Bis(8-quinolyl)-2,3,7,8,12,13,17,18-octaethylporphyrin.** To a solution of 3,3′,4,4′-tetraethyl-2,2′-dipyrrylmethene hydrobromide (326 mg, 0.967 mmol)[23] in ethanol (10 mL) was added under N_2 a solution of $NaBH_4$ (39.7 mg, 1.65 mmol) in ethanol (3 mL) until the reaction mixture turned from dark brown to pale brown. After 1.5 h of stirring at room temperature, the solvent was evaporated, and ether (20 mL) was added to the residue. The precipitate was filtered off, and the filtrate was evaporated to yield 3,3′,4,4′-tetraethyl-2,2′-dipyrrylmethane (246 mg, 0.954 mmol). 3,3′,4,4′-Tetraethyl-2,2′-dipyrrylmethane (246 mg, 0.954 mmol) and 8-formylquinoline (157 mg, 1.00 mmol) were dissolved in methanol (11.5 mL, degassed by N_2 bubbling for 1 h), and a solution of *p*-toluenesulfonic acid monohydrate (59 mg, 0.31 mmol) in methanol (4 mL, degassed) was added dropwise. The reaction mixture was then stirred for 20 h in the dark. After the solvent was evaporated, the residue was dissolved in THF (27.6 mL), followed by the addition of a solution of chloranil (345 mg, 1.4 mmol) in THF (2.8 mL). The solution was stirred for 1.2 h. After the solvent was evaporated, the residue was purified by silica gel column chromatography ($CHCl_3$/acetone = 25:1) to separate the trans and cis isomers. The cis isomer was recrystallized from $CHCl_3$/hexane: UV−vis ($CHCl_3$ containing amylenes) λ_{max} (log ϵ) 416 nm (5.26), 512 nm (4.16), 546 nm (3.63), 579 nm (3.79), 631 nm (3.08); ^{1}H NMR (500 MHz, $CDCl_3$) δ 10.10 (s, 2H), 8.72 (dd, J = 3.7, 1.6 Hz, 2H), 8.47 (dd, J = 8.6, 1.8 Hz, 2H), 8.34 (dd, J = 6.4, 0.9 Hz, 2H), 8.28 (dd, J = 8.5, 1.2 Hz, 2H), 7.84 (dd, J = 8.3, 7.1 Hz, 2H), 7.46 (dd, J = 8.5, 4.0 Hz, 2H), 3.96−3.87 (m, 8H), 2.57−2.50 (m, 4H), 2.43−2.35 (m, 4H), 1.79 (t, J = 7.7 Hz, 12H), 0.76 (t, J = 7.3 Hz, 12H), −1.68 (br, 2H); HRMS calcd for $C_{54}H_{56}N_6$ *m/z* 788.4566, found 788.4597.

[*cis*- and *trans*-5,15-Bis(8-quinolyl)-2,3,7,8,12,13,17,18-octaethylporphyrinato]zinc(II). To the free base porphyrin (11.1 mg, 14.4 μmol) dissolved in $CHCl_3$ (20 mL) was added methanol saturated with zinc acetate (1.5 mL), and the solution was refluxed for 30 min. The reaction mixture was poured to water, and the resultant mixture was extracted with $CHCl_3$. The organic layer was washed with water, dried over Na_2SO_4, and evaporated.

[*cis*-5,15-Bis(8-quinolyl)-2,3,7,8,12,13,17,18-octaethylporphyrinato]zinc(II) (1). The cis isomer was separated via silica gel column chromatography using 17% EtOAc in $CHCl_3$ as an eluent and further purified by recrystallization from $CHCl_3$/hexane. Pure **1** was dried in vacuo at room temperature for over 50 h: UV−vis ($CHCl_3$ containing amylenes) λ_{max} (log ϵ) 417 nm (5.43), 543 nm (4.23), 579 nm (3.97); ^{1}H NMR (500 MHz, $CDCl_3$) 10.11 (s, 2H), 8.59 (dd, J = 4.9, 1.5 Hz, 2H), 8.46 (m, 4H), 8.29 (dd, J = 8.2, 1.5 Hz, 2H), 7.85 (dd, J = 7.0, 8.2 Hz, 2H), 7.41 (dd, J = 8.5, 4.0 Hz, 2H), 3.95−3.83 (m, 8H), 2.51−2.44 (m, 4H), 2.29−2.22 (m, 4H), 1.79 (t, J = 7.6 Hz, 12H), 0.73 (t, J = 7.3 Hz, 12H); HRMS calcd for $C_{54}H_{54}N_6Zn$ *m/z* 850.3702, found 850.3710.

[*trans*-5,15-Bis(8-quinolyl)-2,3,7,8,12,13,17,18-octaethylporphyrinato]zinc(II) (2). The trans isomer was separated by passing through triethylamine pretreated silica gel column using 5% EtOAc in $CHCl_3$ as an eluent and further purified by recrystallization from $CHCl_3$/hexane. Pure **2** was dried in vacuo at room temperature for over 50 h: UV−vis ($CHCl_3$ containing amylenes) λ_{max} (log ϵ) 417 nm (5.45), 543 nm (4.18), 579 nm (3.93); ^{1}H NMR (500 MHz, $CDCl_3$) δ 10.10 (s, 2H), 8.57 (dd, J = 4.0, 1.8 Hz, 2H), 8.55 (dd, J = 6.7, 1.5 Hz, 2H), 8.44 (dd, J = 8.2, 1.8 Hz, 2H), 8.29 (dd, J = 8.2, 1.5 Hz, 2H), 7.88 (dd, J = 8.2, 6.7 Hz, 2H), 7.38 (dd, J = 8.6, 4.0 Hz, 2H), 3.89 (q, J = 7.6 Hz, 8H), 2.48−2.41 (m, 4H), 2.32−2.25 (m, 4H), 1.76 (t, J = 7.6 Hz, 12H), 0.71 (t, J = 7.6 Hz, 12H); HRMS calcd for $C_{54}H_{54}N_6Zn$ *m/z* 850.3702, found 850.3717.

Octyl β-D-Glucopyranoside. Spectroscopic data (Dojindo laboratories, used as received): ^{1}H NMR (500 MHz, 1.7 mM in $CDCl_3$ at 25 °C) δ 4.29 (d, J = 7.6 Hz, 1H, 1-H), 3.93−3.78 (m, 2H), 3.88 (dt, J = 9.5, 6.7 Hz, 1H, CH_3-$(CH_2)_6$-CH_2O-), 3.61−3.48 (m, 2H), 3.51 (dt, J = 9.5, 7.0 Hz, 1H, CH_3-$(CH_2)_6$-CH_2O-), 3.41−3.32 (m, 2H), 2.62 (d, J = 2.1 Hz, 1H, 3-OH), 2.50 (d, J = 2.8 Hz, 1H, 4-OH), 2.37 (d, J = 2.1 Hz, 1H, 2-OH), 1.96 (t, J = 7.0 Hz, 1H, 6-OH), 1.61 (m, 2H, CH_3-$(CH_2)_5CH_2$-CH_2O-), 1.26 (m, 10H, CH_3-$(CH_2)_5CH_2$-CH_2O-), 0.86 (t, J = 7.0 Hz, 3H, CH_3-$(CH_2)_6$-CH_2O-).

Octyl α-D-Glucopyranoside. Spectroscopic data (Sigma, used as received): ^{1}H NMR (500 MHz, 1.9 mM in $CDCl_3$ at 25 °C) δ 4.85 (d, J = 4.0 Hz, 1H, 1-H), 3.87−3.78 (m, 2H), 3.74−3.62 (m, 2H), 3.71 (dt, J = 9.5, 6.5 Hz, 1H, CH_3-$(CH_2)_6$-CH_2O-), 3.57−3.53 (m, 1H), 3.48−3.40 (m, 1H), 3.43 (dt, J = 9.0, 7.0 Hz, 1H, CH_3-$(CH_2)_6$-CH_2O-), 2.55 (d, J = 2.1 Hz, 1H, 3-OH), 2.47 (d, J = 2.8 Hz, 1H, 4-OH), 1.97 (d, J = 10.7 Hz, 1H, 2-OH), 1.89 (dd, J = 7.0, 5.5 Hz, 1H, 6-OH), 1.58 (m, 2H, CH_3-$(CH_2)_5CH_2$-CH_2O-), 1.26 (m, 10H, CH_3-$(CH_2)_5CH_2$-CH_2O-), 0.87 (t, J = 7.0 Hz, 3H, CH_3-$(CH_2)_6$-CH_2O-).

Octyl β-D-Galactopyranoside. This compound was synthesized by the literature procedure.[24] Obtained crude product was purified via silica gel column chromatography (EtOAc/MeOH = 6:1). Further purification was done by recrystallizing from EtOH/hexane. The crystals were completely dried at 60 °C under reduced pressure for 100 h: ^{1}H NMR (500 MHz, 2.5 mM in $CDCl_3$ at 25 °C) δ 4.24 (d, J = 7.3 Hz, 1H, 1-H), 4.01−3.95 (m, 2H), 3.93−3.85 (m, 2H), 3.66−3.58 (m, 2H), 3.55−3.48 (m, 2H), 2.78 (d, J = 2.4 Hz, 1H, 4-OH), 2.61 (d, J = 4.6 Hz, 1H, 3-OH), 2.38 (d, J = 1.8 Hz, 1H, 2-OH), 2.09 (dd, J = 7.9, 4.9 Hz, 1H, 6-OH), 1.62 (m, 2H, CH_3-$(CH_2)_5CH_2$-CH_2O-), 1.27 (m, 10H, CH_3-$(CH_2)_5CH_2$-CH_2O-), 0.86 (t, J = 7.3 Hz, 3H, CH_3-$(CH_2)_6$-CH_2O-); ^{13}C NMR (125.65 MHz, DMSO-d_6) δ 103.47 (1-C), 75.09, 73.51, 70.56, 68.47, 68.13, 60.40, 31.29, 29.37, 28.91, 28.73, 25.57, 22.11, 13.95. Anal. Calcd for $C_{14}H_{28}O_6$: C, 57.51; H, 9.65. Found: C, 57.30; H, 9.88.

Octyl α-D-Galactopyranoside. This compound was obtained as a complex mixture by the literature procedure.[26] The crude product was then passed through a Dowex 1 × 2 (OH form, Dow Chemical Co.) chromatographic column (EtOH/MeOH = 1:1) to give the pure α-anomer, which was completely dried at 60 °C under reduced pressure for 100 h: ^{1}H NMR (500 MHz, 2.3 mM in $CDCl_3$ at 25 °C) δ 4.94 (d, J = 3.7 Hz, 1H, 1-H), 4.08 (m, 1H, 4-H), 3.98−3.94 (m, 1H, 5-H), 3.87−3.69 (m, 4H), 3.71 (dt, J = 9.8, 6.7 Hz, 1H, CH_3-$(CH_2)_6$-CH_2O-), 3.44 (dt, J = 9.5, 6.7 Hz, 1H, CH_3-$(CH_2)_6$-CH_2O-), 2.80 (d, J = 0.6 Hz, 1H, 4-OH), 2.53 (d, J = 3.7 Hz, 1H, 3-OH), 2.20 (dd, J = 7.9, 4.6 Hz, 1H, 6-OH), 1.88 (d, J = 10.4 Hz, 1H, 2-OH), 1.59 (m, 2H, CH_3-$(CH_2)_5CH_2$-CH_2O-), 1.27 (m, 10H, CH_3-$(CH_2)_5CH_2$-CH_2O-), 0.86 (t, J = 7.3 Hz, 3H, CH_3-$(CH_2)_6$-CH_2O-); ^{13}C NMR (125.65 MHz, DMSO-d_6) δ 98.84 (1-C), 71.14, 69.58, 68.84, 68.37, 66.88, 60.57, 31.25, 29.11, 28.84, 28.68, 25.71, 22.07, 13.94. Anal. Calcd for $C_{14}H_{28}O_6$: C, 57.51; H, 9.65. Found: C, 57.21; H, 9.48.

Octyl β-D-Mannopyranoside. This compound was synthesized by the literature procedure.[25] The obtained product was further purified by a Dowex 1 × 2 (OH form, Dow Chemical Co.) chromatographic column (EtOH/MeOH = 2:1). The product was completely dried at 60 °C under reduced pressure for 100 h: ^{1}H NMR (500 MHz, 0.6 mM in $CDCl_3$ at 25 °C) δ 4.52 (d, J = 1.2 Hz, 1H, 1-H), 3.99 (m, 1H), 3.95−3.87 (m, 2H), 3.85−3.80 (m, 1H), 3.76−3.72 (m, 1H), 3.55−3.47 (m, 2H), 3.30−3.26 (m, 1H), 2.47 (d, J = 9.5 Hz, 1H, 3-OH),

(23) Mizutani, T.; Murakami, T.; Kurahashi, T.; Ogoshi, H. *J. Org. Chem.* **1996**, *61*, 539.

(24) Matsumura, S.; Imai, K.; Yoshikawa, S.; Kawada, K.; Uchibori, T. *J. Am. Oil Chem. Soc.* **1990**, *67*, 996.

(25) Kaur, K. J.; Hindsgaul, O. *Glycoconjugate J.* **1991**, *8*, 90.

(26) Konradsson, P.; Roberts, C.; Fraser-Reid, B. *Recl. Trav. Chim. Pays-Bas* **1991**, *110*, 23.

2.42 (d, J = 2.8 Hz, 1H, 4-OH), 2.36 (d, J = 2.4 Hz, 1H, 2-OH), 2.04 (t, J = 6.7 Hz, 1H, 6-OH), 1.60 (m, 2H, CH_3-$(CH_2)_5CH_2$-CH_2O-), 1.26 (m, 10H, CH_3-$(CH_2)_5CH_2$-CH_2O-), 0.86 (t, J = 7.0 Hz, 3H, CH_3-$(CH_2)_6$-CH_2O-); ^{13}C NMR (125.65 MHz, DMSO-d_6) δ 100.22 (1-C), 77.49, 73.71, 70.56, 68.36, 67.17, 61.37, 31.23, 29.18, 28.86, 28.68, 25.58, 22.06, 13.94; Anal. Calcd for $C_{14}H_{28}O_6$: C, 57.51; H, 9.65. Found: C, 57.24; H, 9.81.

Octyl α-D-Mannopyranoside. This compound was obtained as a complex mixture by the literature procedure.[26] The crude product was then passed through a Dowex 1 × 2 (OH form, Dow Chemical Co.) chromatographic column (EtOH/MeOH = 2:1) to give the pure α-anomer, which was completely dried at 60 °C under reduced pressure for 100 h: ^{1}H NMR (500 MHz, 0.3 mM in $CDCl_3$ at 25 °C) δ 4.82 (d, J = 1.5 Hz, 1H, 1-H), 3.93 (m, 1H), 3.89−3.77 (m, 4H), 3.68−3.61 (m, 1H), 3.66 (dt, J = 9.5, 6.7 Hz, 1H, CH_3-$(CH_2)_6$-CH_2O-), 3.39 (dt, J = 9.5, 6.4 Hz, 1H, CH_3-$(CH_2)_6$-CH_2O-), 2.37 (d, J = 5.5 Hz, 1H, 3-OH), 2.34 (d, J = 3.1 Hz, 1H, 4-OH), 2.19 (d, J = 4.6 Hz, 1H, 2-OH), 1.99 (t, J = 6.7 Hz, 1H, 6-OH), 1.55 (m, 2H, CH_3-$(CH_2)_5CH_2$-CH_2O-), 1.25 (m, 10H, CH_3-$(CH_2)_5CH_2$-CH_2O-), 0.87 (t, J = 7.3 Hz, 3H, CH_3-$(CH_2)_6$-CH_2O-); ^{13}C NMR (125.65 MHz, DMSO-d_6) δ 99.70 (1-C), 73.91, 71.00, 70.39, 66.97, 66.17, 61.26, 31.23, 28.97, 28.77, 28.66, 25.73, 22.05, 13.93. Anal. Calcd for $C_{14}H_{28}O_6$: C, 57.51; H, 9.65. Found: C, 57.27; H, 9.82.

Octyl 6-*O*-Benzoyl-β-D-glucopyranoside. To a solution of octyl β-D-glucopyranoside (155 mg, 0.52 mmol) and pyridine (3.7 mL) in dichloromethane (3.0 mL) was added benzoyl chloride (144 mg, 1.03 mmol) in dichloromethane (6.0 mL) dropwise over 6 h at −40 °C. After the reaction mixture was allowed to warm to room temperature over 12 h, excess benzoyl chloride was decomposed by the addition of MeOH. The solvent was evaporated, and the residue was purified by column chromatography on silica gel (ether/acetone = 4:1) to obtain octyl 6-*O*-benzoyl-β-D-glucopyranoside (43.9 mg, 0.11 mmol, 22%): ^{1}H NMR (500 MHz, $CDCl_3$) δ 8.07−7.43 (m, 5H, benzoyl-H), 4.75 (dd, J = 12.2, 4.6 Hz, 1H, 6-H), 4.53 (dd, J = 12.2, 2.2 Hz, 1H, 6-H), 4.30 (d, J = 7.7 Hz, 1H, 1-H), 3.89 (dt, J = 9.4, 7.7 Hz, 1H, CH_3-$(CH_2)_6$-CH_2O-), 3.61 (t, J = 9.1 Hz, 1H, 3-H), 3.57 (m, 1H, 5-H), 3.52 (dt, J = 9.6, 7.0 Hz, 1H, CH_3-$(CH_2)_6$-CH_2O-), 3.48 (m, 1H, 4-H), 3.38 (dd, J = 9.5, 8.0 Hz, 1H, 2-H), 3.14 (s, 1H, 4-OH), 2.81 (s, 1H, 3-OH), 2.46 (s, 1H, 2-OH), 1.64−1.59 (m, 2H, CH_3-$(CH_2)_5CH_2$-CH_2O-), 1.28−1.24 (m, 10H, CH_3-$(CH_2)_5CH_2$-CH_2O-), 0.87 (t, J = 5.5 Hz, 3H, CH_3-$(CH_2)_6$-CH_2O-); HRMS calcd for $C_{21}H_{33}O_7$ *m/z* 397.2226, found 397.2237.

Octyl 6-*O*-Acetyl-β-D-glucopyranoside. To a solution of octyl β-D-glucopyranoside (152 mg, 0.51 mmol) and pyridine (3.7 mL) in dichloromethane (3.0 mL) was added acetyl chloride (80 mg, 1.0 mmol) in dichloromethane (6.0 mL) dropwise over 6 h at −40 °C. After the reaction mixture was allowed to warm to room temperature over 12 h, excess acetyl chloride was decomposed by the addition of MeOH. The solvent was evaporated. The residue was purified by column chromatography on silica gel (ether/acetone = 4:1) to obtain octyl 6-*O*-acetyl-β-D-glucopyranoside (52.6 mg, 0.16 mmol, 31%): ^{1}H NMR (500 MHz, $CDCl_3$) δ 4.55−4.51 (dd, J = 12.5, 4.7 Hz, 1H, 6-H), 4.27 (d, J = 7.8 Hz, 1H, 1-H), 4.25 (dd, J = 12.5, 2.5 Hz, 1H, 6-H), 3.90 (dt, J = 24.7, 19.4 Hz, 1H, CH_3-$(CH_2)_6$-CH_2O-), 3.58 (m, 1H, 3-H), 3.50 (dt, J = 24.7, 19.4 Hz, 1H, CH_3-$(CH_2)_6$-CH_2O-), 3.44 (m, 1H, 5-H), 3.39 (m, 2H, 2-H and 4-H), 3.02 (s, 1H, 4-OH), 2.78 (s, 1H, 3-OH), 2.43 (s, 1H, 2-OH), 2.21 (s, 3H, CH_3CO_2-), 1.65−1.57 (m, 2H, CH_3-$(CH_2)_5CH_2$-CH_2O-), 1.37−1.21 (m, 10H, CH_3-$(CH_2)_5CH_2$-CH_2O-), 0.87 (t, J = 5.4 Hz, 3H, CH_3-$(CH_2)_6$-CH_2O-); HRMS calcd for $C_{16}H_{31}O_7$ *m/z* 335.2056, found 335.2063.

Synthesis of Octyl 2-*O*-Methyl-α-D-mannopyranoside. Mannose Pentaacetate. Mannose pentaacetate was prepared from mannose and anhydrous sodium acetate in acetic anhydride by the reported procedure.[27] The obtained product was a mixture of α- and β-anomers and a small amount of straight-chain mannose peracetate. Since separation was quite difficult, this mixture was subjected to the next reaction after passing through a silica gel column (hexane/EtOAc = 1:1).

Octyl 2,3,4,6-Tetra-*O*-acetyl-α-D-mannopyranoside. This pyranoside was obtained stereoselectively by a modified procedure of S. Matsumura *et al.*,[24] in which 1.2 equiv of silver trifluoromethanesulfonate was used instead of silver carbonate and 3.2 equiv of tetramethylurea was added together with octanol and silver trifluoromethanesulfonate to minimize orthoester formation. Purification was done by silica gel column chromatography (hexane/EtOAc = 2:1). The yield was 43%: ^{1}H NMR (500 MHz, $CDCl_3$) δ 5.28 (m, 1H), 5.04 (m, 1H), 4.84 (s, 1H), 4.27 (m, 1H), 4.12−3.88 (m, 3H), 3.65 (m, 1H), 3.44 (m, 1H), 2.09−2.00 (m, 12H), 1.55 (m, 2H), 1.24 (m, 10H), 0.87 (t, J = 7.0 Hz, 3H).

Octyl α-D-Mannopyranoside. Deacetylation was carried out by the reported procedure.[25] Less than 1% of β-anomer was detected by ^{1}H NMR. The product was passed through a silica gel column (EtOAc/MeOH = 9:1) and was used for the next reaction. The yield was 92%: ^{1}H NMR (500 MHz, 0.3 mM in $CDCl_3$ at 25 °C) δ 4.82 (d, J = 1.5 Hz, 1H, 1-H), 3.93 (m, 1H), 3.89−3.77 (m, 4H), 3.68−3.61 (m, 1H), 3.66 (dt, J = 9.5, 6.7 Hz, 1H, CH_3-$(CH_2)_6$-CH_2O-), 3.39 (dt, J = 9.5, 6.4 Hz, 1H, CH_3-$(CH_2)_6$-CH_2O-), 2.37 (d, J = 5.5 Hz, 1H, 3-OH), 2.34 (d, J = 3.1 Hz, 1H, 4-OH), 2.19 (d, J = 4.6 Hz, 1H, 2-OH), 1.99 (t, J = 6.7 Hz, 1H, 6-OH), 1.55 (m, 2H, CH_3-$(CH_2)_5CH_2$-CH_2O-), 1.25 (m, 10H, CH_3-$(CH_2)_5CH_2$-CH_2O-), 0.87 (t, J = 7.3 Hz, 3H, CH_3-$(CH_2)_6$-CH_2O-); ^{13}C NMR (125.65 MHz, DMSO-d_6) δ 99.70 (1-C), 73.92, 71.00, 70.40, 66.97, 66.17, 61.26, 31.24, 28.98, 28.78, 28.68, 25.75, 22.07, 13.94.

Octyl 4,6-*O*-Benzylidene-α-D-mannopyranoside. Benzylidenation was effected by $PhCH(OMe)_2HBF_4{\cdot}OEt_2$.[28] The temperature was kept at −40 °C during the reaction and gradually increased to room temperature. The crude product was purified by silica gel column chromatography (hexane/EtOAc = 8:5) and further purified by recrystallization from hexane/EtOAc. The yield was 67%: ^{1}H NMR (500 MHz, $CDCl_3$) δ 7.49−7.47 (m, 2H), 7.38−7.34 (m, 3H), 5.56 (s, 1H), 4.85 (d, J = 1.2 Hz, 1H, 1-H), 4.26 (m, 1H), 4.10−4.03 (m, 2H), 3.91 (m, 1H), 3.84−3.79 (m, 2H), 3.68 (dt, J = 9.8, 6.7 Hz, 1H), 3.41 (dt, J = 9.5, 6.7 Hz, 1H), 2.54 (d, J = 2.1 Hz, 1H, OH), 2.53 (d, J = 3.4 Hz, 1H, OH), 1.59−1.51 (m, 2H), 1.27 (m, 10H), 0.87 (t, J = 7.0 Hz, 3H).

Octyl 4,6-*O*-Benzylidene-3-*O*-benzyl-α-D-mannopyranoside. The procedure reported by Boger *et al.*[29] was used for selective benzylation of the equatorial 3-OH group of octyl 4,6-*O*-benzylidene-α-D-mannopyranoside. The crude product was purified by silica gel column chromatography (hexane/EtOAc = 4:1). The yield was 81%: ^{1}H NMR (500 MHz, $CDCl_3$) δ 7.50−7.47 (m, 2H), 7.37−7.27 (m, 8H), 5.60 (s, 1H, benzylidene-H), 4.85 (d, J = 11.9 Hz, 1H, benzyl-H), 4.84 (d, J = 1.5 Hz, 1H, 1-H), 4.71 (d, J = 11.9 Hz, 1H, benzyl-H), 4.25 (m, 1H), 4.08 (m, 1H), 4.04 (m, 1H, 2-H), 3.92 (dd, J = 9.5, 3.0 Hz, 1H, 3-H), 3.85−3.81 (m, 2H), 3.67 (dt, J = 9.5, 7.0 Hz, 1H, CH_3-$(CH_2)_6$-CH_2O-), 3.38 (dt, J = 9.5, 7.0 Hz, 1H, CH_3-$(CH_2)_6$-CH_2O-), 2.63 (d, J = 1.5 Hz, 1-H, 2-OH), 1.55 (m, 2H, CH_3-$(CH_2)_5CH_2$-CH_2O-), 1.26 (m, 10H, CH_3-$(CH_2)_5CH_2$-CH_2O-), 0.87 (t, J = 7.5 Hz, 3H, CH_3-$(CH_2)_6$-CH_2O-).

Octyl 4,6-*O*-Benzylidene-3-*O*-benzyl-2-*O*-methyl-α-D-mannopyranoside. The procedure for methylation of benzyl 3,4,6-tri-*O*-benzyl-β-L-glucopyranoside[30] was found to be effective for methylation of octyl 4,6-*O*-benzylidene-3-*O*-benzyl-α-D-mannopyranoside. The crude product was purified by silica gel column chromatography (hexane/EtOAc = 4:1). The yield was 89%: ^{1}H NMR (500 MHz, $CDCl_3$) δ 7.45−7.42 (m, 2H), 7.32−7.19 (m, 8H), 5.55 (s, 1H), 4.82 (d, J = 12.2 Hz, 1H), 4.76 (d, J = 1.2 Hz, 1H), 4.65 (d, J = 12.2 Hz, 1H), 4.17 (dd, J = 10.1, 4.3 Hz, 1H), 4.08 (dd, J = 9.8, 9.8 Hz, 1H), 3.89 (dd, J = 10.1, 3.4 Hz, 1H), 3.79 (dd, J = 10.1, 10.1 Hz, 1H), 3.71 (dt, J = 4.6, 9.5 Hz, 1H), 3.59 (dt, J = 9.5, 7.0 Hz, 1H), 3.52 (dd, J = 3.1, 1.5 Hz, 1H), 3.49 (s, 3H), 3.32 (dt, J = 9.8, 6.7 Hz, 1H), 1.50 (m, 2H), 1.22 (m, 10H), 0.82 (t, J = 7.0 Hz, 3H).

Octyl 2-*O*-Methyl-α-D-mannopyranoside. Removal of both the benzyl group and the benzylidene group was done by catalytic transfer hydrogenation reported by Hanessian *et al.*[31] The crude product was purified first by silica gel column chromatography (EtOAc/MeOH =

(27) Rosevear, P.; VanAken, T.; Baxter, J.; Ferguson-Miller, S. *Biochemistry* **1980**, *19*, 4108.

(28) Albert, R.; Dax, K.; Pleschko, R.; Stutz, A. E. *Carbohydr. Res.* **1985**, *137*, 282.

(29) Boger, D. L.; Honda, T. *J. Am. Chem. Soc.* **1994**, *116*, 5647.

(30) Boger, D. L.; Teramoto, S.; Zhou, J. *J. Am. Chem. Soc.* **1995**, *117*, 7344.

(31) Hanessian, S.; Liak, T. J.; Vanasse, B. *Synthesis* **1981**, 396.

9:1) and then by passing through a Dowex 1 × 2 (OH form, Dow Chemical Co.) chromatographic column using methanol as an eluent. The pure product was obtained in a 98% yield as hygroscopic liquid: ^{1}H NMR (500 MHz, $CDCl_3$) δ 4.89 (d, J = 1.2 Hz, 1H, 1-H), 3.87−3.74 (m, 3H), 3.67 (dt, J = 9.8, 6.7 Hz, 1H, CH_3-$(CH_2)_6$-CH_2O-), 3.65 (m, 1H, 4-H), 3.58 (m, 1H, 5-H), 3.46 (s, 3H, CH_3O-), 3.45 (dd, J = 1.5 Hz, 1H, 2-H), 3.38 (dt, J = 9.5, 6.4 Hz, 1H, CH_3-$(CH_2)_6$-CH_2O-), 2.45 (d, J = 2.7 Hz, 1H, 4-OH), 2.29 (d, J = 10.4 Hz, 1H, 3-OH), 2.02 (dd, J = 7.0, 5.8 Hz, 1H, 6-OH), 1.56 (m, 2H, CH_3-$(CH_2)_5CH_2$-CH_2O-), 1.26 (m, 10H, CH_3-$(CH_2)_5CH_2$-CH_2O-), 0.87 (t, J = 7.3 Hz, 3H, CH_3-$(CH_2)_6$-CH_2O-); ^{13}C NMR (125.65 MHz, DMSO-d_6) δ 96.51 (1-C), 80.57, 73.96, 70.88, 67.24, 66.35, 61.15, 58.55, 31.24, 29.00, 28.78, 28.67, 25.74, 22.08, 13.94. Anal. Calcd for $C_{15}H_{30}O_6 \cdot {}^1/_4H_2O$: C, 57.95; H, 9.89. Found: C, 58.03; H, 9.82.

UV−Vis Titrations and CD Spectral Measurements. Binding constants were determined by UV−vis titrations. To avoid the influence by the ethanol added as a stabilizer to chloroform, amylene-containing chloroform was used throughout the study. The water concentration was estimated to be about 0.002% from ^{1}H NMR. The atropisomerization from the cis isomer (**1**) to the trans isomer (**2**) in a $CDCl_3$ solution occurred slowly: 5% of **1** was isomerized to **2** at room temperature for 100 h although no isomerization was observed in the solid state. Therefore, the receptor solution was prepared just before use. Cis to trans isomerization in receptors **3** and **4** was too slow to observe.

The details of the determination of the binding constant are as follows. To *ca.* 5 × 10^{-6} M of **1**−**5** in $CHCl_3$ was added a stock solution of carbohydrate ligands in $CHCl_3$ at 15 °C. The changes in absorbance at around 424 nm in the Soret band were monitored at eight different concentrations of carbohydrate, with volume change due to carbohydrate addition being taken into account during analysis. Assuming 1:1 complexation, the binding constants were evaluated by a least-squares parameter estimation based on the damping Gauss−Newton method. Calculated curves were well fitted to absorbance changes.

It was reported that glycopyranosides aggregate when dissolved in organic solvent at a high concentration.[8] The UV−vis titration experiments of **1** and **2** were performed in the low-concentration range of the ligands, where no aggregation occurs. For the binding of Man by receptors **3** and **4**, at the highest concentration of Man, aggregation occurred. However the standard deviations of binding constants of these receptor−ligand complexes were 6−10%, comparable to those for other complexes, showing that the errors owing to the ligand aggregation were negligibly small.

^{1}H NMR Study of Binding. $CDCl_3$ was completely deacidified by passing through alumina (basic, activity super 1, ICN) just before use. To 0.3−0.8 mM of carbohydrate in $CDCl_3$ was added a stock solution of **1** or **2** in $CDCl_3$ at 25 °C, and the complexation-induced shifts of signals for carbohydrates were recorded. The concentration of **1** or **2** was kept considerably low ($[H-G]/[G]_{total} < 20\%$) to avoid signal broadening. The CIS values were determined by extrapolating the chemical shift to 100% complex, based on the concentrations of the complex calculated from K determined by UV−vis titration.

Acknowledgment. We thank T. Kobatake for his kind help in the mass spectroscopy measurements. This work was supported by a Grant-in Aid for Scientific Research from the Ministry of Education, Science, Sports, and Culture, Japan.

JA9713183